AD-A103 202 ARMY COMMUNICATIONS-ELECTRONICS ENGINEERING INSTALLAT--ETC F/G 9/1
SIMPLIFIED SOLUTIONS TO THE ELECTRICAL PROPERTIES OF LINEAR CYL--ETC(U)
MAY 80 H F TOLLES
UNCLASSIFIED CCC-EMEO-PED-80-4

END
DATE
FILMED
9-81
DTIC

Electromagnetics Engineering Office
Propagation Engineering Division
Technical Report EMEO-PED-80-4



# SIMPLIFIED SOLUTIONS TO THE ELECTRICAL PROPERTIES OF LINEAR CYLINDRICAL ANTENNA ELEMENTS NEAR FIRST RESONANCE

BY

HAROLD F. TOLLES

May 1980

DISTRIBUTION STATEMENT:
Approved for public release;
distribution unlimited.



HEADQUARTERS
US ARMY COMMUNICATIONS-ELECTRONICS
ENGINEERING INSTALLATION AGENCY
Fort Huachuca, Arizona 85613

DEPARTMENT OF THE ARMY
US ARMY COMMUNICATIONS-ELECTRONICS
ENGINEERING INSTALLATION AGENCY
ELECTROMAGNETICS ENGINEERING OFFICE
Fort Huachuca, Arizona 85613

This Technical Report was prepared by the Propagation Engineering Division, Electromagnetics Engineering Office, of the Communications-Electronics Engineering Installation Agency and is published for the information and guidance of all addressees. Suggestions and criticism relative to the form, contents, purpose, or use of this publication should be referred to the attention of the Commander, US Army Communications-Electronics Engineering Installation Agency, ATTN: CCC-EMEO-PED, Fort Huachuca, Arizona 85613. Technical comments may be coordinated directly with the authors, at (602) 538-6779 or AUTOVON 879-6779.

MILES A. MERKEL
Chief, Electromagnetics Engineering Office

Electromagnetics Engineering Office
Propagation Engineering Division
Technical Report EMEO-PED-80-4

# SIMPLIFIED SOLUTIONS TO THE ELECTRICAL PROPERTIES OF LINEAR CYLINDRICAL ANTENNA ELEMENTS NEAR FIRST RESONANCE

BY

HAROLD F. TOLLES

May 1980

DISTRIBUTION STATEMENT:
Approved for public release;
distribution unlimited.

HEADQUARTERS
US ARMY COMMUNICATIONS-ELECTRONICS
ENGINEERING INSTALLATION AGENCY
Fort Huachuca, Arizona 85613

UNCLASSIFIED

SECURITY CLASSIFICATION OF THIS PAGE (When Data Entered)

| REPORT DOCUMENTATION PAGE | | READ INSTRUCTIONS BEFORE COMPLETING FORM |
|---|---|---|
| 1. REPORT NUMBER<br>Tech Rpt No. EMEO-PED-80-4 | 2. GOVT ACCESSION NO. | 3. RECIPIENT'S CATALOG NUMBER |
| 4. TITLE (and Subtitle)<br>Simplified Solutions to the Electrical Properties of Linear Cylindrical Antenna Elements Near First Resonance | | 5. TYPE OF REPORT & PERIOD COVERED<br>6. PERFORMING ORG. REPORT NUMBER |
| 7. AUTHOR(s)<br>Harold F. Tolles | | 8. CONTRACT OR GRANT NUMBER(s) |
| 9. PERFORMING ORGANIZATION NAME AND ADDRESS<br>Commander<br>USACEEIA, ATTN: CCC-EMEO-PED<br>Fort Huachuca, Arizona 85613 | | 10. PROGRAM ELEMENT, PROJECT, TASK AREA & WORK UNIT NUMBERS |
| 11. CONTROLLING OFFICE NAME AND ADDRESS<br>HQUSACEEIA<br>ATTN: CCC-EMEO-PED<br>Fort Huachuca, Arizona 85613 | | 12. REPORT DATE<br>May 1980<br>13. NUMBER OF PAGES<br>Thirty-nine (39) |
| 14. MONITORING AGENCY NAME & ADDRESS (if different from Controlling Office) | | 15. SECURITY CLASS. (of this report)<br>UNCLASSIFIED<br>15a. DECLASSIFICATION/DOWNGRADING SCHEDULE |

16. DISTRIBUTION STATEMENT (of this Report)

DISTRIBUTION STATEMENT: Approved for public release; distribution unlimited.

17. DISTRIBUTION STATEMENT (of the abstract entered in Block 20, if different from Report)

18. SUPPLEMENTARY NOTES

19. KEY WORDS (Continue on reverse side if necessary and identify by block number)

20. ABSTRACT (Continue on reverse side if necessary and identify by block number)

DD FORM 1 JAN 73 1473 EDITION OF 1 NOV 65 IS OBSOLETE

UNCLASSIFIED

SECURITY CLASSIFICATION OF THIS PAGE (When Data Entered)

TABLE OF CONTENTS



RE: Distribution Statement, Technical Report
EMEO-PED-80-4
Unlimited per Mr. H. F. Tolles, ACEEIA/CCC-
EMEO-PED

A

# I. INTRODUCTION

One of the missions of CCC-EMEO-PED is to provide customers with antenna modeling performance data. To carry out this mission, we obtained the AMP (Antenna Modeling Program) in 1972, the NEC (Numerical Electromagnetic Code - Method of Moments) Program in 1977, and the new NEC (NEC with Sommerfeld integral subroutine) Program in January of this year.

A review of much data over the years reveals different solutions when the two programs are used, and useful simplifications can be developed for linear elements when excited near first resonance (e.g., dipole). The differences are discussed and simplified equations are presented in this report.

Graphical solutions are presented, and they show that these equations are highly comparable when a center-fed antenna element, L, is between 0.40 and 0.55 wavelength long. This enables one to verify computer programs, and to obtain many key solutions without having to resort to complex programs on large computers such as CDC-6500/6600.

Some of the equations and graphs were developed from $\beta_0 h$ point data where,

$$\beta_0 h = \pi \frac{L}{\lambda} \doteq 0.010479 \; (Lf_{MHz}) \qquad \text{radians}$$

In this form, they relate directly to the theoretical work by Drs. King and Middleton which is often used as the reference. Being developed from point data, the coefficients of the equations are range weighted, and other coefficients can be used to shift the accuracy range of these simple equation forms.

## II. COMPARISONS

A review of mode theory[1], King-Middleton theory[2], AMP program, NEC program, and Dr. J. Lawson theory[3] results shows varying degrees of agreement. For example, the relative velocity factor at first resonance in terms of element length divided by diameter ,L/D, ratio for these 5 examples can be obtained from the following approximate equations in the same order.

$$V_{r_o} \doteq 1 - [11.293 \log_{10} (\tfrac{L}{D}) - 9.767]^{-1} \qquad \text{numeric} \quad 1$$

$$V_{r_o} \doteq 1 - [10.1 \log_{10} (\tfrac{L}{D}) - 2.0]^{-1} \qquad \text{numeric} \quad 2$$

$$V_{r_o} \doteq 1 - [12.4 \log_{10} (\tfrac{L}{D}) - 7.0]^{-1} \qquad \text{numeric} \quad 3$$

$$V_{r_o} \doteq 1 - [11.541 \log_{10} (\tfrac{L}{D}) - 4.933]^{-1} \qquad \text{numeric} \quad 4$$

$$V_{r_o} \doteq 1 - [10.7575 \log_{10} (\tfrac{L}{D}) - 8.0]^{-1} \qquad \text{numeric} \quad 5$$

These equations are plotted on Figure 1. Surprisingly, the NEC results are essentially between those of the other two pairs while both AMP and NEC programs use the King-Wu 3-term element current distribution[4]. In addition, series-fed scaling experience a number of years ago with $50 < \frac{L}{D} < 200$ indicates that the NEC results are more accurate than those of the other 4. . .even though the AMP results better match those by King-Middleton!

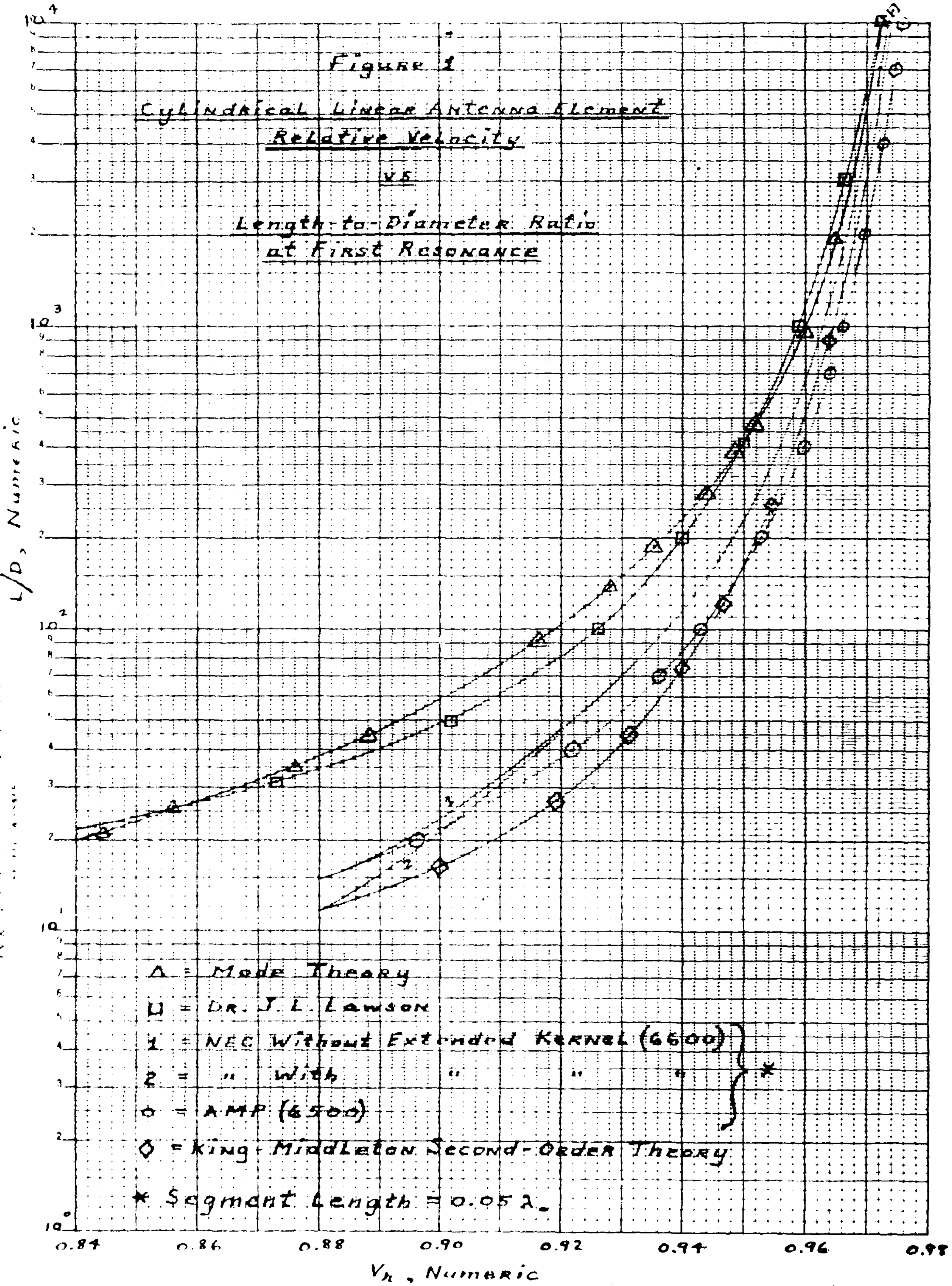

Figure 1
Cylindrical Linear Antenna Element
Relative Velocity
vs
Length-to-Diameter Ratio
at First Resonance
L/D, Numeric
Vr, Numeric
0.84
0.86
0.88
0.90
0.92
0.94
0.96
0.98
Δ = Mode Theory
□ = Dr. J. L. Lawson
1 = NEC Without Extended Kernel (6500)
2 = " With " " "
○ = AMP (6500)
◇ = King-Middleton Second-Order Theory
* Segment Length = 0.05λ

The first resonance radiation resistance in terms of element length divided by diameter ,L/D, ratio for these 5 examples can be obtained from the following approximate equations in the same order.

$$R_{res} \doteq 73.0 - [0.055 \log_{10}(\frac{L}{D}) - 0.019]^{-1} \quad \text{ohms} \quad 6$$

$$R_{res} \doteq 73.0 - [0.315 \log_{10}(\frac{L}{D}) - 0.214]^{-1} \quad \text{ohms} \quad 7$$

$$R_{res} \doteq 73.0 - [0.054 \log_{10}(\frac{L}{D}) + 0.62]^{-1} \quad \text{ohms} \quad 8$$

$$R_{res} \doteq 73.0 - [0.252 \log_{10}(\frac{L}{D}) + 0.232]^{-1} \quad \text{ohms} \quad 9$$

$$R_{res} = 73.0 \quad \text{ohms} \quad 10$$

With the exception of equation 10, these equations are plotted on Figure 2. The results vividly illustrate the problems associated with obtaining valid radiation resistance solutions vs. element length divided by diameter, L/D, ratio discussed in reference 1.

I find no other reference that believes radiation resistance is independent of L/D. Hence, equation 10 is not correct. The mode theory and King-Middleton theory curves on Figure 2 do not consider series feed gap capacitance or the method of connecting transmission lines. The AMP and NEC programs use the center segment to series drive the entire antenna element and, therefore, must make allowances for gap effects. These allowances can not be deduced from program printouts because current distribution-thus impedance-is related to all segment sizes. That is, the effects are interrelated, and best answers are obtained when each segment length is near 0.05 free-space wavelengths[5]. Since theoretical

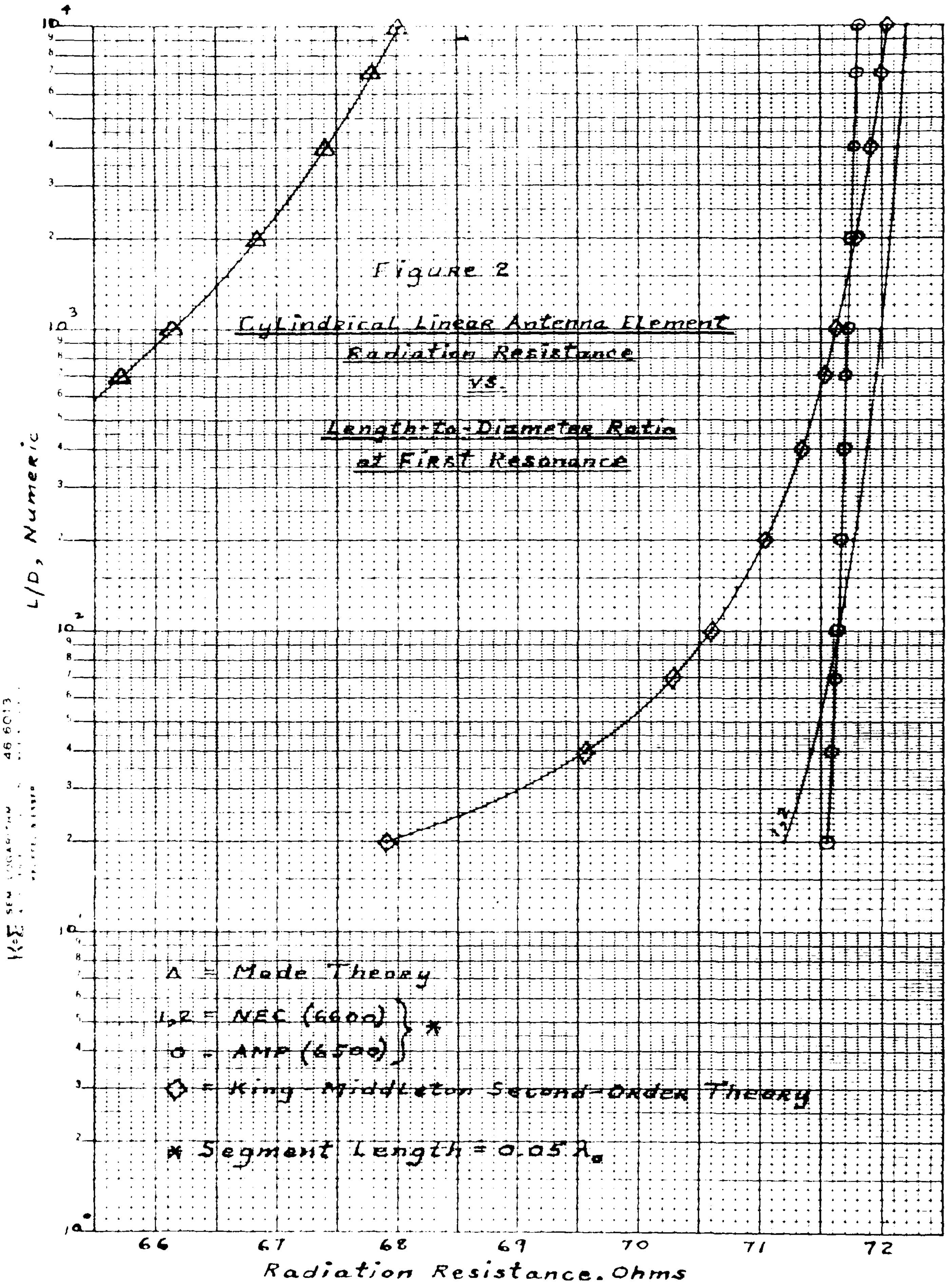

Figure 2
Cylindrical Linear Antenna Element
Radiation Resistance
vs.
Length-to-Diameter Ratio
at First Resonance
Δ = Mode Theory
1,2 = NEC (6600)
o = AMP (6500)
* 
◇ = King-Middleton Second-Order Theory
* Segment Length = 0.05 λ₀
L/D, Numeric
Radiation Resistance. Ohms
66
67
68
69
70
71
72

approximations are used in the programs, inclusion of lengthy source equations in this report does not seem to be warranted.

Field experience indicates that the mode-theory curve on Figure 2 generally gives too low an input resistance when shunt-excited, and that the series-fed configuration is more sensitive to L/D changes than the AMP results indicate. Too, I suggest that some of the measurements reported in reference 1 may have included ground mutual coupling impedance without realizing it. The selection of resistance values is highly critical in scaling applications.

Prior to the 1950's, most of the driven antenna elements were series-fed. It is convenient, VSWR tolerant, and vacuum tubes can handle relatively large voltage transients. When solid-state amplifiers became popular, it soon became apparent that they could be destroyed by antenna element voltage buildups when the element was insulated and series-fed. This brought a renaissance of delta, tee, and gamma antenna matching networks because they can be used to shunt-excite a center-grounded element. This, together with center-grounded passive reflector/director array elements, makes it desirable to have valid impedances for both the series-fed and shunt-excited antenna element.

Based upon these observations, the best data base we have at this time is King-Middleton for solid elements and NEC for split series-fed elements. AMP results are available, but are not included. They are not as accurate, and this program is not available at this time. Additional mode theory calculations were not made because of their relative inaccuracy. They can be obtained from equation 108, page 433, of reference 1.

## III. SOLID ELEMENT CENTER-FED INPUT IMPEDANCE

Using the available L/D together with $1.2 \leq \beta_0 h \leq 1.8$ King-Middleton data points[2], the radiation resistance of the solid element may be obtained from:

$$R_r = 10^p \qquad \text{ohms} \qquad 11$$

where,

$$p = [1.023 - 0.035 \log_{10}(\frac{L}{D})](\beta_0 h) + 0.034 \log_{10}(\frac{L}{D}) + 0.368 \qquad \text{numeric}$$

Equation 11 is not very accurate when $(L/D) \leq 45$. When $(L/D) > 45$, this equation is within 3.0 ohms for all 42 data points, within 2.0 ohms for 39 data points, and within 1.0 *ohm* near first resonance.

Using the available L/D together with $1.2 \leq \beta_0 h \leq 1.8$ King-Middleton data points[2], the *input reactance* of the solid element may be obtained from:

$$X_r = [288.225 \log_{10}(\frac{L}{D}) - 91.504](\beta_0 h) - 451.793 \log_{10}(\frac{L}{D}) + 184.045 \qquad \text{ohms} \qquad 12$$

*Equation* 12 is not very accurate when $(L/D) \leq 45$. When $(L/D) > 45$, this equation is within 6.0 ohms for all 42 data points, within 2.0 ohms for 41 data points, and within 1.0 ohm near first resonance.

When equations 11 and 12 are used to obtain $M/\underline{\theta}$, the deviation from King-Middleton results is less than 2.4% in M and 1.75 in degrees for all 42 data points.

## IV. SPLIT SERIES CENTER-FED ELEMENT INPUT IMPEDANCE

Using 11 L/D together with $1.2 \leq \beta_0 h \leq 1.8$ data points in the NEC program, the radiation resistance of the split center-fed element may be obtained from:

$$R_r = 10^p \qquad \text{ohms} \qquad 13$$

where,

$$p = \left[0.984-0.049 \log_{10}\left(\frac{L}{D}\right)\right](\beta_0 h)+0.043 \log_{10}\left(\frac{L}{D}\right)+0.470 \qquad \text{numeric}$$

Equation 13 is not very accurate when (L/D) < 40. When (L/D) $\geq$ 40, this equation is within 7.0 ohms for all 77 data points, within 3.0 ohms for 65 data points, and within 1.5 ohms near first resonance.

Using 11 L/D together with $1.2 \leq \beta_0 h \leq 1.8$ data points in the NEC program, the input reactance of the split center-fed element may be obtained from:

$$X_r = \left[288.274 \log_{10}\left(\frac{L}{D}\right)-77.434\right](\beta_0 h)-455.916 \log_{10}\left(\frac{L}{D}\right)+175.298 \qquad \text{ohms} \qquad 14$$

Equation 14 is not very accurate when (L/D) < 40. When (L/D) $\geq$ 40, this equation is within 12.0 ohms for all 77 data points, within 3.0 ohms for 61 data points, and within 2.0 ohms near first resonance.

When equations 13 and 14 are used to obtain M $\underline{/\theta}$, the deviation from NEC results is less than 4.5% in M and 3.3 in degrees for all 77 data points.

The NEC data points are questionable. As pointed out in Section II, best answers are obtained when each segment length is near 0.05 free-space wavelengths, and this is the case here, near first resonance. It was not done for the other $\beta_0 h$ values of interest because this would have increased the program usage and reduction time manifold. Therefore, equations 13 and 14 may be more or less accurate than indicated. This should not be alarming because program accuracy is sometimes no better than $\pm$ 10%.

## V. ELEMENT SCALING

As indicated by the above equations, $R_r$ and $X_r$ solutions are a function of L/D and $L(\lambda_0)$, and they are unique. That is, when L/D and $L(\lambda_0)$ are given, only one value of $R_r$ and $X_r$ exist for each configuration, and individual term scaling is not possible. At the same time, ratios of $X_r/R_r$ can be scaled, and it is the ratio that is so important in electrical scaling[2].

Using the available L/D together with $1.2 \leq \beta_0 h \leq 1.8$ King-Middleton data points[2], the ratio for the solid element may be obtained from:

$$\frac{X_r}{R_r} = \left[2.4312 - \frac{1.5252}{\beta_0 h - 0.9356}\right] \log_{10}\left(\frac{L}{D}\right) + \frac{2.7413}{\beta_0 h - 0.6341} - 2.5202 \quad \text{numeric} \qquad (15)$$

Equation 15 is not very accurate when (L/D) < 45. When (L/D) $\geq$ 45, this equation is within 2.89 electrical degrees * for all 42 data points, and within 2.0 electrical degrees for 38 of the data points.

Equation 15 is plotted on Figures 3KM - 7KM in terms of L in conventional free-space wavelengths for direct use. The dotted lines are King-Middleton solutions near the maximum useful range of equation 15. They show that equation 15 is surprisingly accurate when 0.40 < L < 0.55 wavelengths!

Using 11 L/D together with $1.2 < \beta_0 h < 1.8$ data points in the NEC program, the ratio for the split center-fed element may be obtained from:

$$\frac{X_r}{R_r} = \left[2.6636 - \frac{1.7863}{\beta_0 h - 0.8991}\right] \log_{10}\left(\frac{L}{D}\right) + \frac{4.0258}{\beta_0 h - 0.5101} - 3.2649 \quad \text{numeric} \qquad 16$$

Equation 16 is not very accurate when (L/D) < 40. When (L/D) $\geq$ 40, this equation is within 3.14 electrical degrees * for all 77 data points, and within 2.0 electrical degrees for 73 of the data points.

Equation 16 is plotted on Figures 8N - 12N in terms of L in conventional free-space wavelengths for direct use. The dotted lines are NEC solutions near the maximum useful range of equation 16. They show that equation 16 is surprisingly accurate when 0.40 < L < 0.55 wavelengths!

* $\theta_e = \tan^{-1}\left(\frac{X}{R}\right)$ degrees

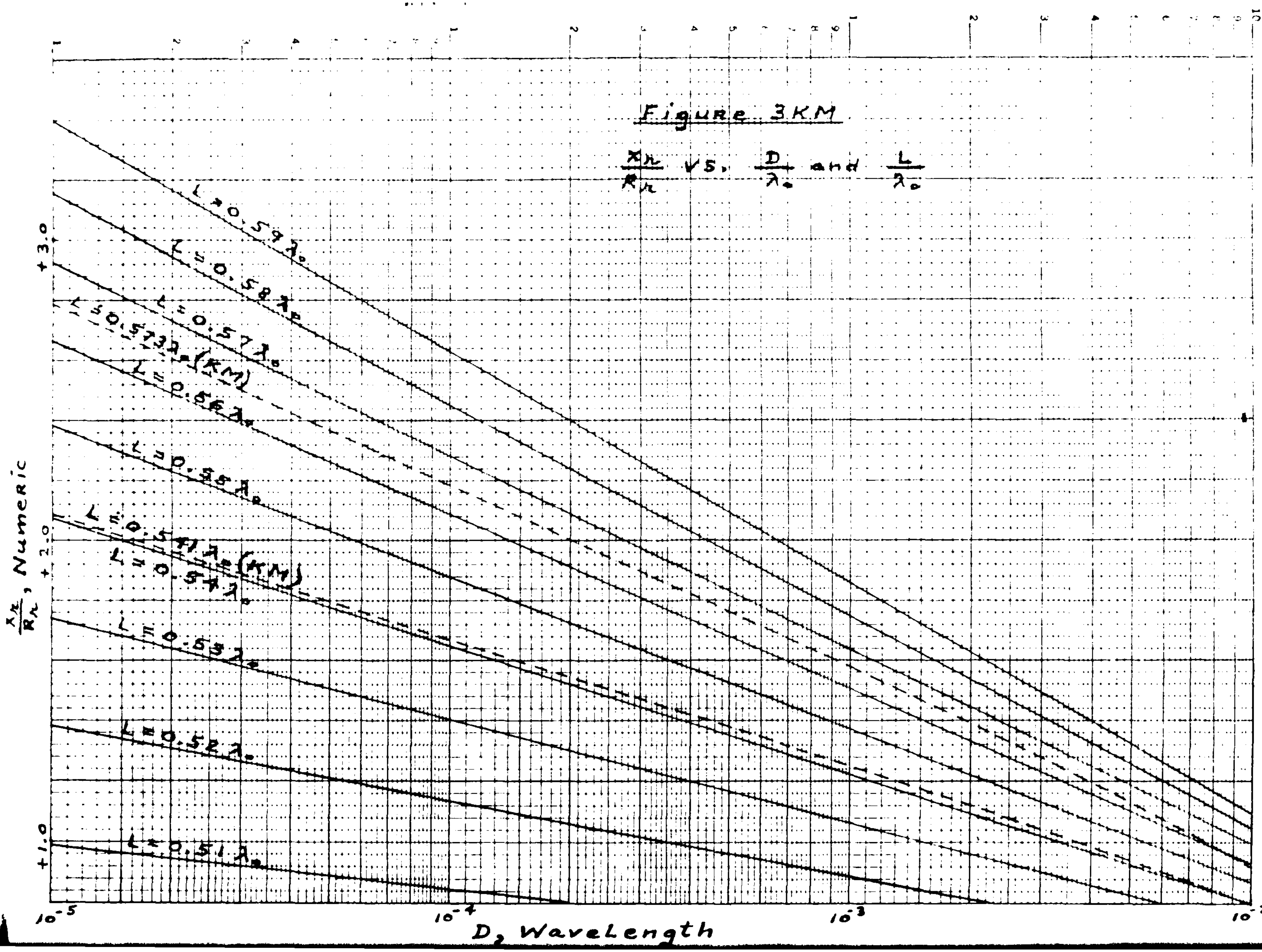

Figure 3KM
$\frac{X_n}{R_n}$ vs. $\frac{D}{\lambda_0}$ and $\frac{L}{\lambda_0}$
$L = 0.59\lambda_0$
$L = 0.58\lambda_0$
$L = 0.57\lambda_0$
$L = 0.5733\lambda_0$ (KM)
$L = 0.56\lambda_0$
$L = 0.55\lambda_0$
$L = 0.541\lambda_0$ (KM)
$L = 0.54\lambda_0$
$L = 0.53\lambda_0$
$L = 0.52\lambda_0$
$L = 0.51\lambda_0$
+3.0
+2.0
+1.0
$10^{-5}$
$10^{-4}$
$10^{-3}$
$10^{-2}$
$\frac{X_n}{R_n}$, Numeric
D, Wavelength

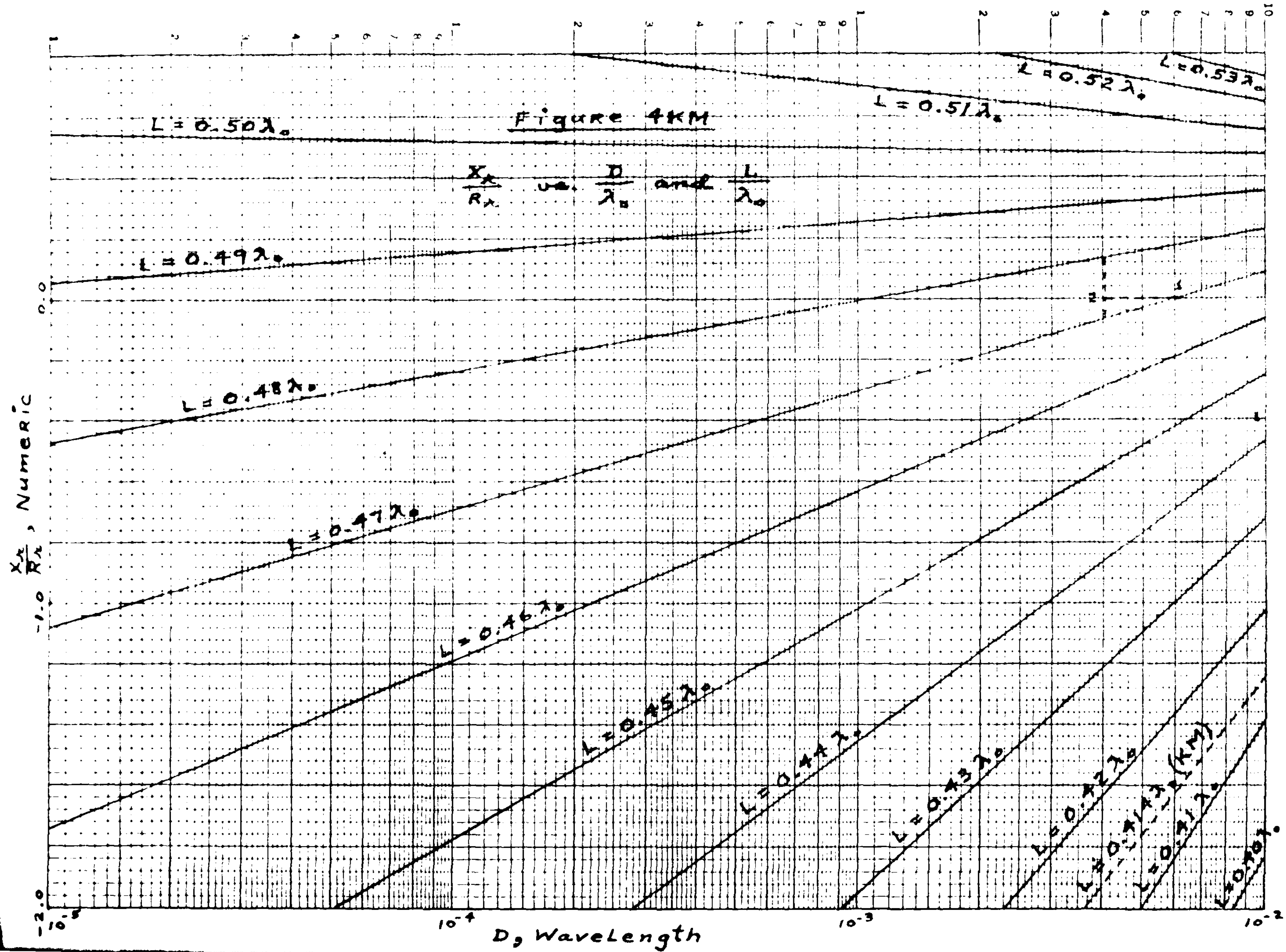

Figure 4KM
$\frac{X_r}{R_r}$ vs. $\frac{D}{\lambda_0}$ and $\frac{L}{\lambda_0}$
L = 0.53λ₀
L = 0.52λ₀
L = 0.51λ₀
L = 0.50λ₀
L = 0.49λ₀
L = 0.48λ₀
L = 0.47λ₀
L = 0.46λ₀
L = 0.45λ₀
L = 0.44λ₀
L = 0.43λ₀
L = 0.42λ₀
L = 0.41λ₀ (KM)
L = 0.41λ₀
L = 0.40λ₀
0.0
-1.0
-2.0
$10^{-5}$
$10^{-4}$
$10^{-3}$
$10^{-2}$
D, Wavelength
$\frac{X_r}{R_r}$, Numeric

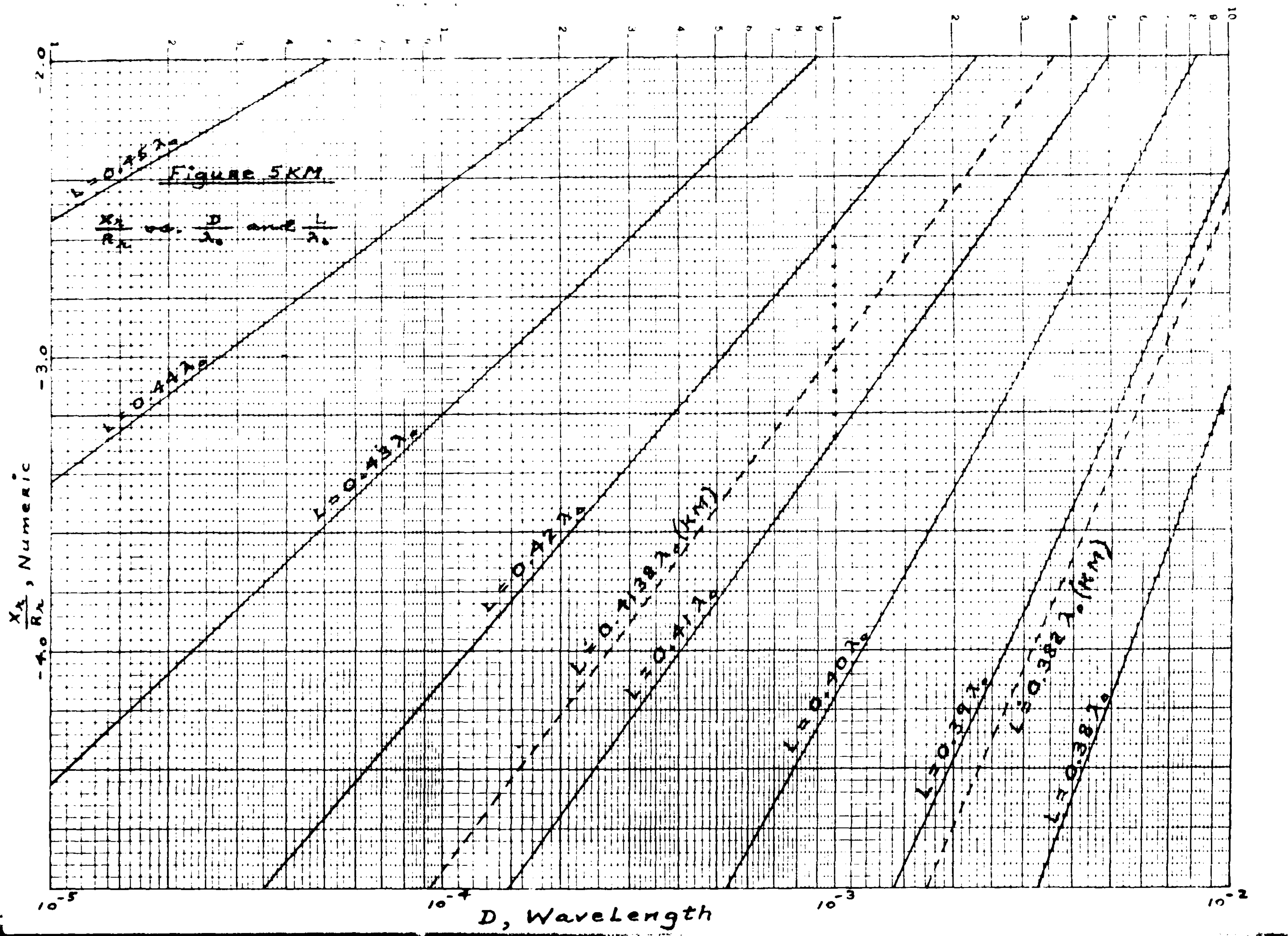

Figure 5KM
$\frac{X_\lambda}{R_\lambda}$ vs. $\frac{D}{\lambda_0}$ and $\frac{L}{\lambda_0}$
$L = 0.45\lambda_0$
$L = 0.44\lambda_0$
$L = 0.43\lambda_0$
$L = 0.42\lambda_0$
$L = 0.4138\lambda_0$ (KM)
$L = 0.41\lambda_0$
$L = 0.40\lambda_0$
$L = 0.39\lambda_0$
$L = 0.382\lambda_0$ (KM)
$L = 0.38\lambda_0$
-2.0
-3.0
-4.0
$\frac{X_\lambda}{R_\lambda}$, Numeric
$10^{-5}$
$10^{-4}$
$10^{-3}$
$10^{-2}$
D, Wavelength

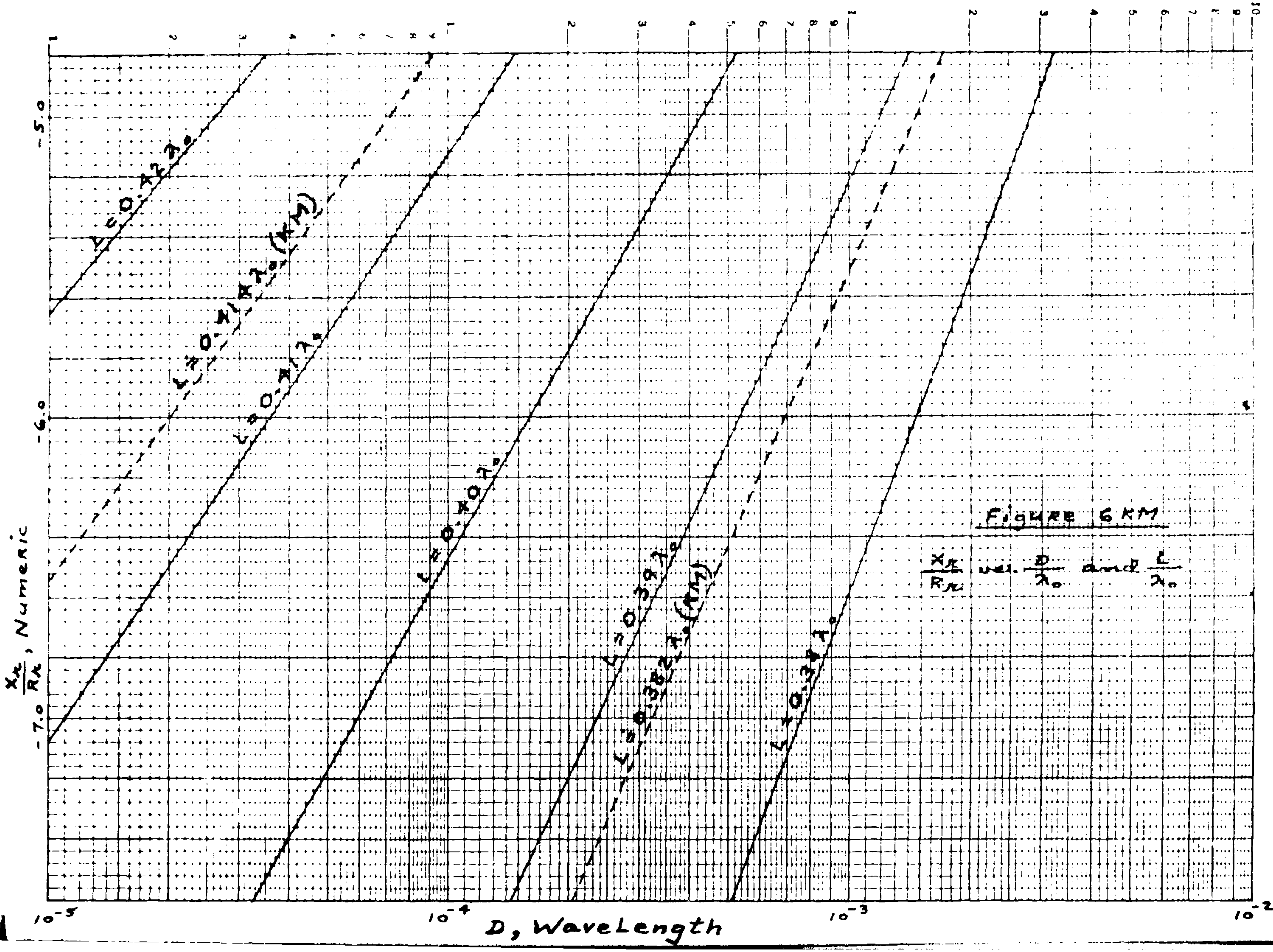

FIGURE 6KM
$\frac{X_R}{R_R}$ vs. $\frac{D}{\lambda_0}$ and $\frac{L}{\lambda_0}$
D, WaveLength
$\frac{X_R}{R_R}$, Numeric
$10^{-5}$
$10^{-4}$
$10^{-3}$
$10^{-2}$
-5.0
-6.0
-7.0

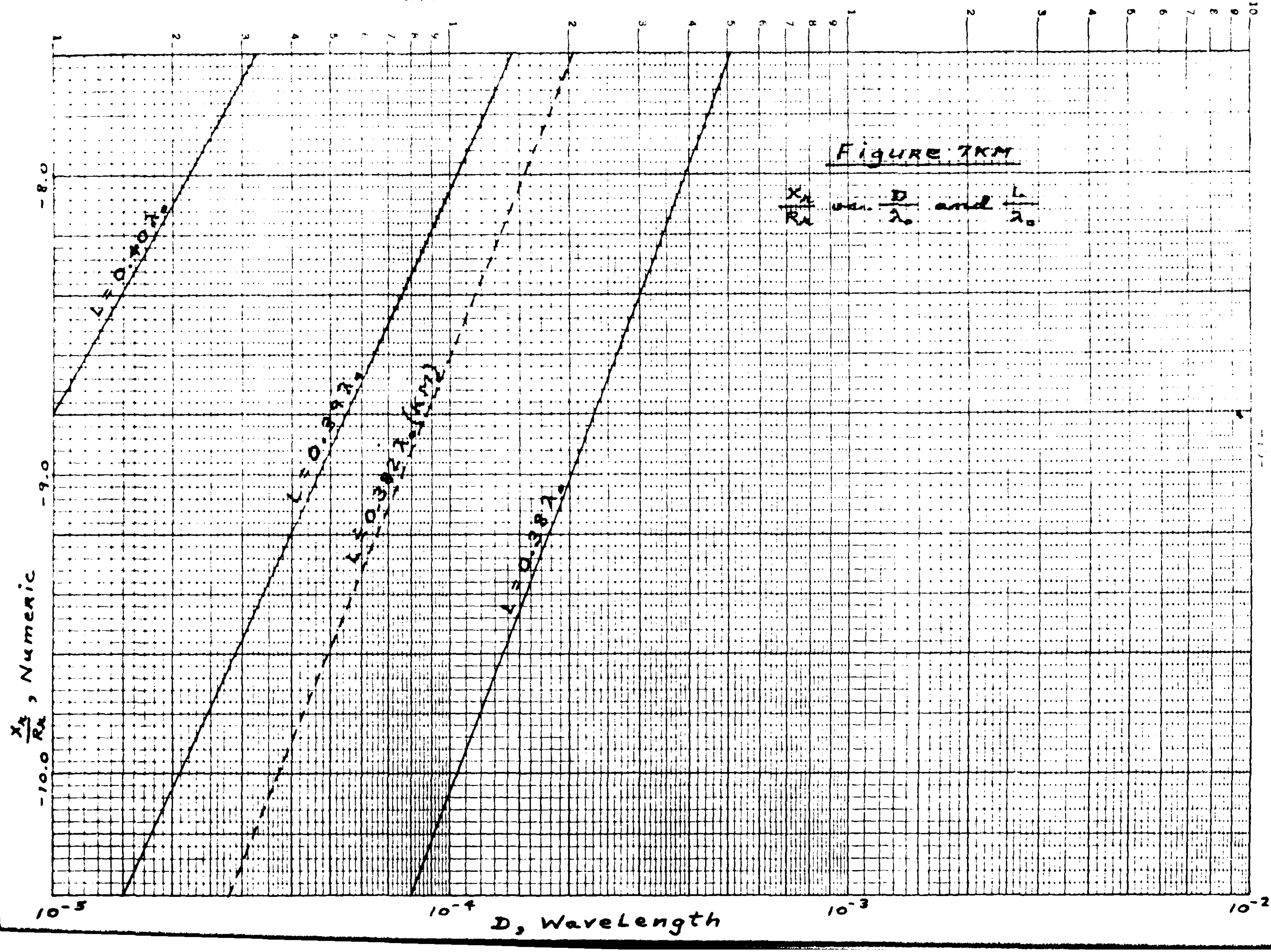
Figure 7KM
$\frac{X_A}{R_A}$ vs. $\frac{D}{\lambda_0}$ and $\frac{L}{\lambda_0}$
-8.0
-9.0
-10.0
$\frac{X_A}{R_A}$, Numeric
$10^{-5}$
$10^{-4}$
$10^{-3}$
$10^{-2}$
D, Wavelength

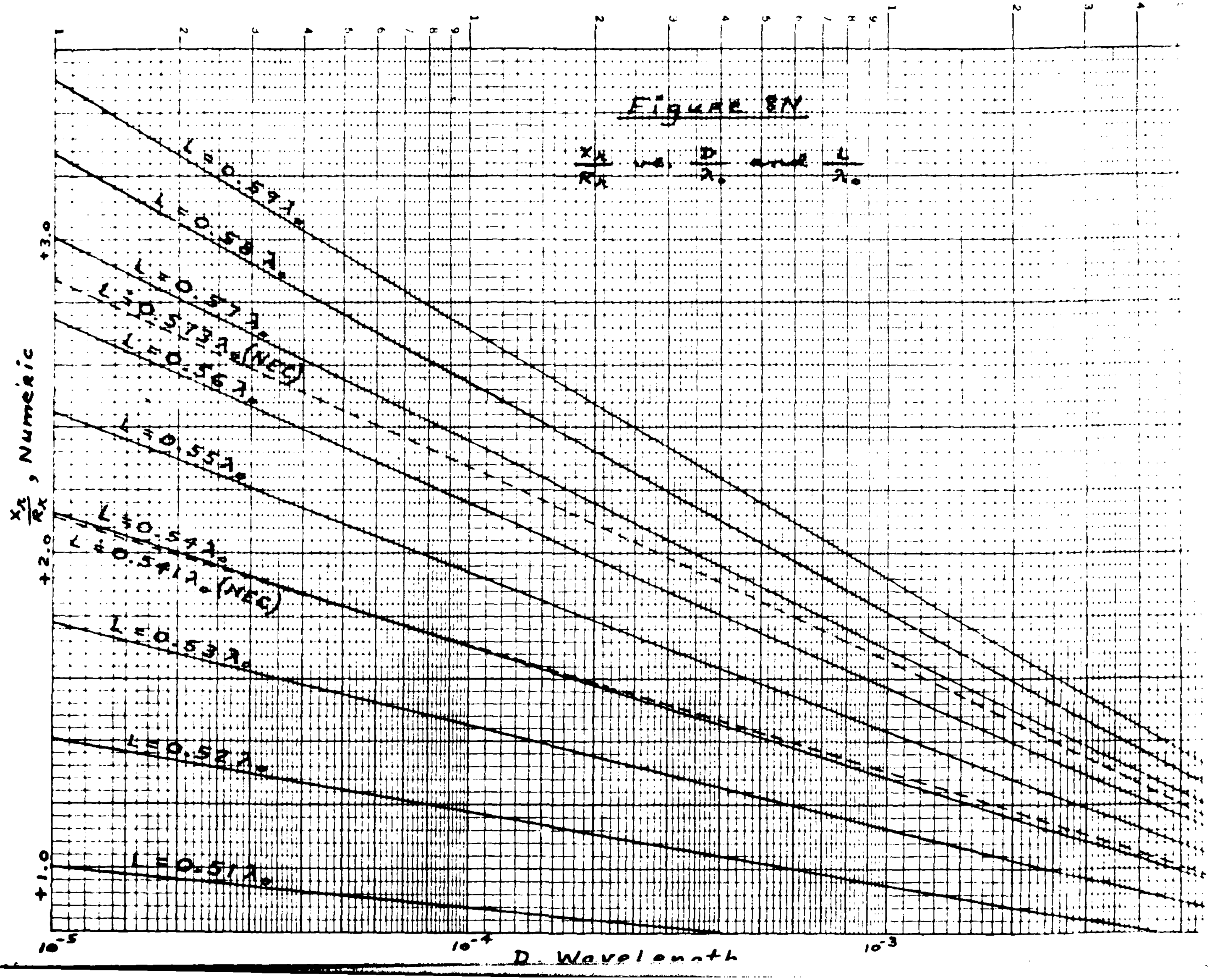

Figure 8N
$\frac{X_A}{R_A}$ vs. $\frac{D}{\lambda_0}$ and $\frac{L}{\lambda_0}$
L = 0.59 λo
L = 0.58 λo
L = 0.57 λo
L = 0.573 λo (NEC)
L = 0.56 λo
L = 0.55 λo
L = 0.54 λo
L = 0.541 λo (NEC)
L = 0.53 λo
L = 0.52 λo
L = 0.51 λo
+3.0
+2.0
+1.0
$\frac{X_A}{R_A}$, Numeric
$10^{-5}$
$10^{-4}$
$10^{-3}$
D Wavelength

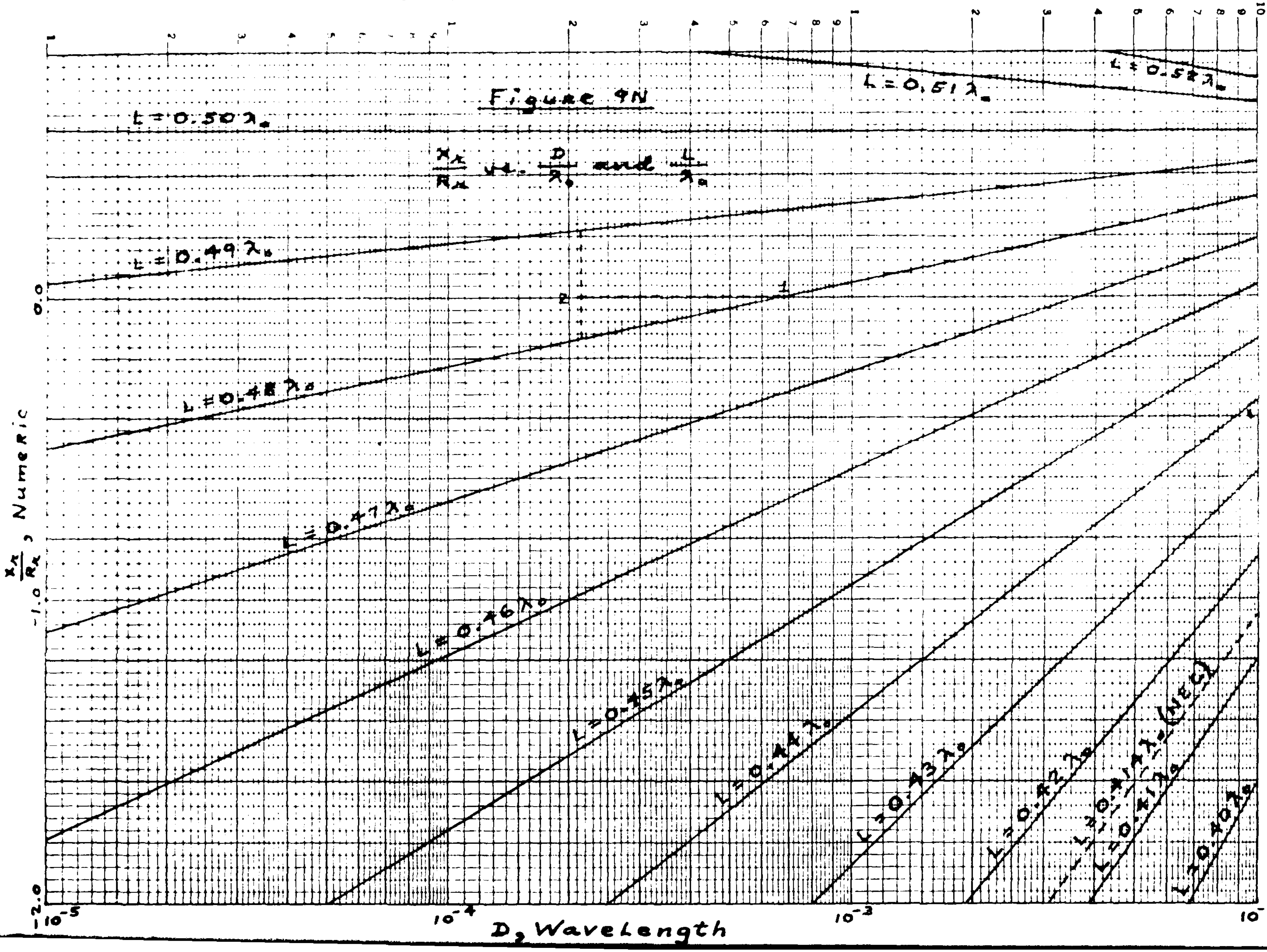

Figure 9N
$\frac{X_A}{R_A}$ vs. $\frac{D}{\lambda_0}$ and $\frac{L}{\lambda_0}$
$L = 0.52\lambda_0$
$L = 0.51\lambda_0$
$L = 0.50\lambda_0$
$L = 0.49\lambda_0$
$L = 0.48\lambda_0$
$L = 0.47\lambda_0$
$L = 0.46\lambda_0$
$L = 0.45\lambda_0$
$L = 0.44\lambda_0$
$L = 0.43\lambda_0$
$L = 0.42\lambda_0$
$L = 0.414\lambda_0$ (NEC)
$L = 0.41\lambda_0$
$L = 0.40\lambda_0$
$\frac{X_A}{R_A}$, Numeric
0.0
-1.0
-2.0
D, Wavelength
$10^{-5}$
$10^{-4}$
$10^{-3}$
$10^{-2}$

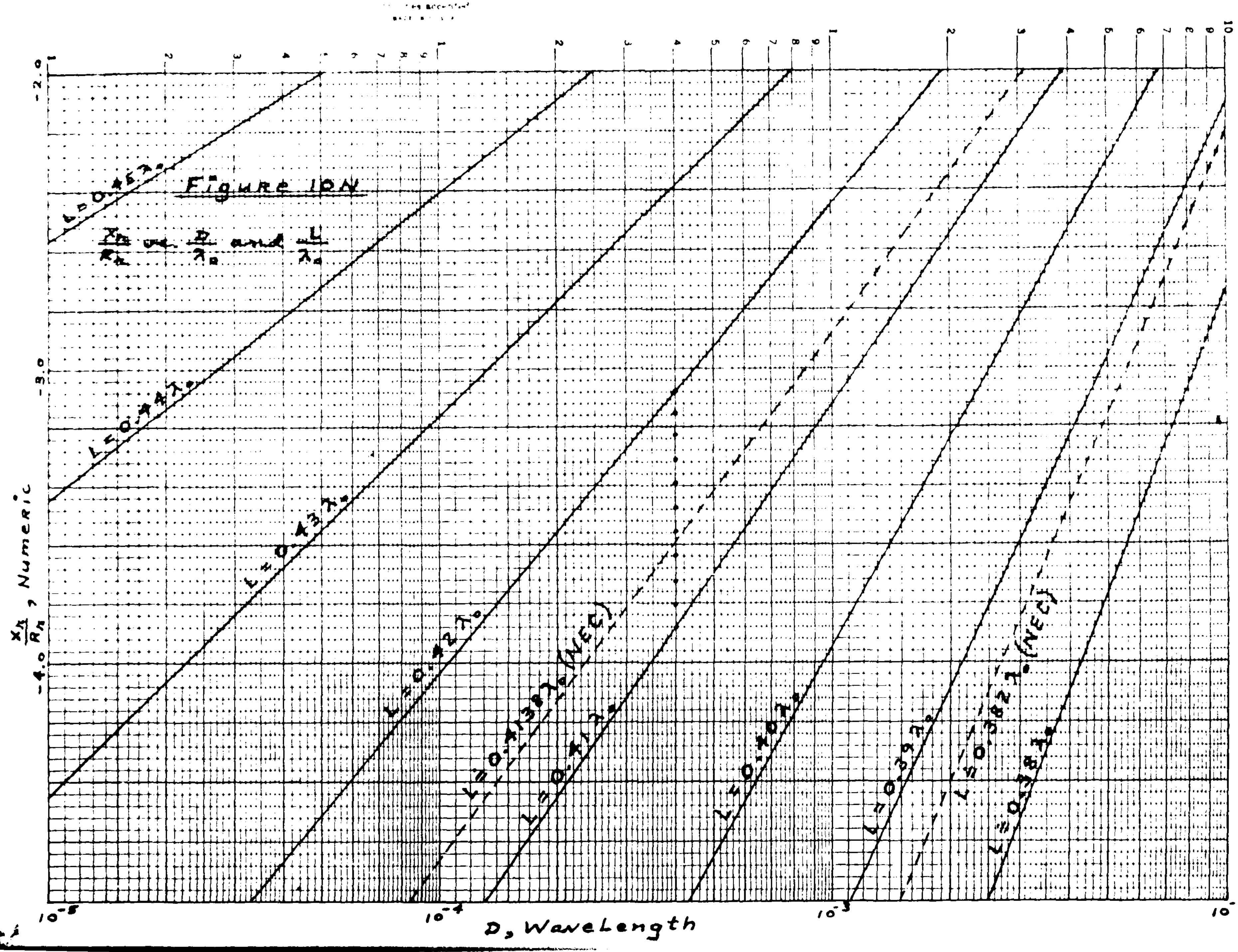

Figure 10N
$\frac{X_n}{R_n}$ vs. $\frac{D}{\lambda_o}$ and $\frac{L}{\lambda_o}$
L = 0.45 λo
L = 0.44 λo
L = 0.43 λo
L = 0.42 λo
L = 0.4138 λo (NEC)
L = 0.41 λo
L = 0.40 λo
L = 0.39 λo
L = 0.382 λo (NEC)
L = 0.38 λo
-2.0
-3.0
-4.0
$\frac{X_n}{R_n}$, Numeric
D, WaveLength
$10^{-5}$
$10^{-4}$
$10^{-3}$
$10^{-2}$

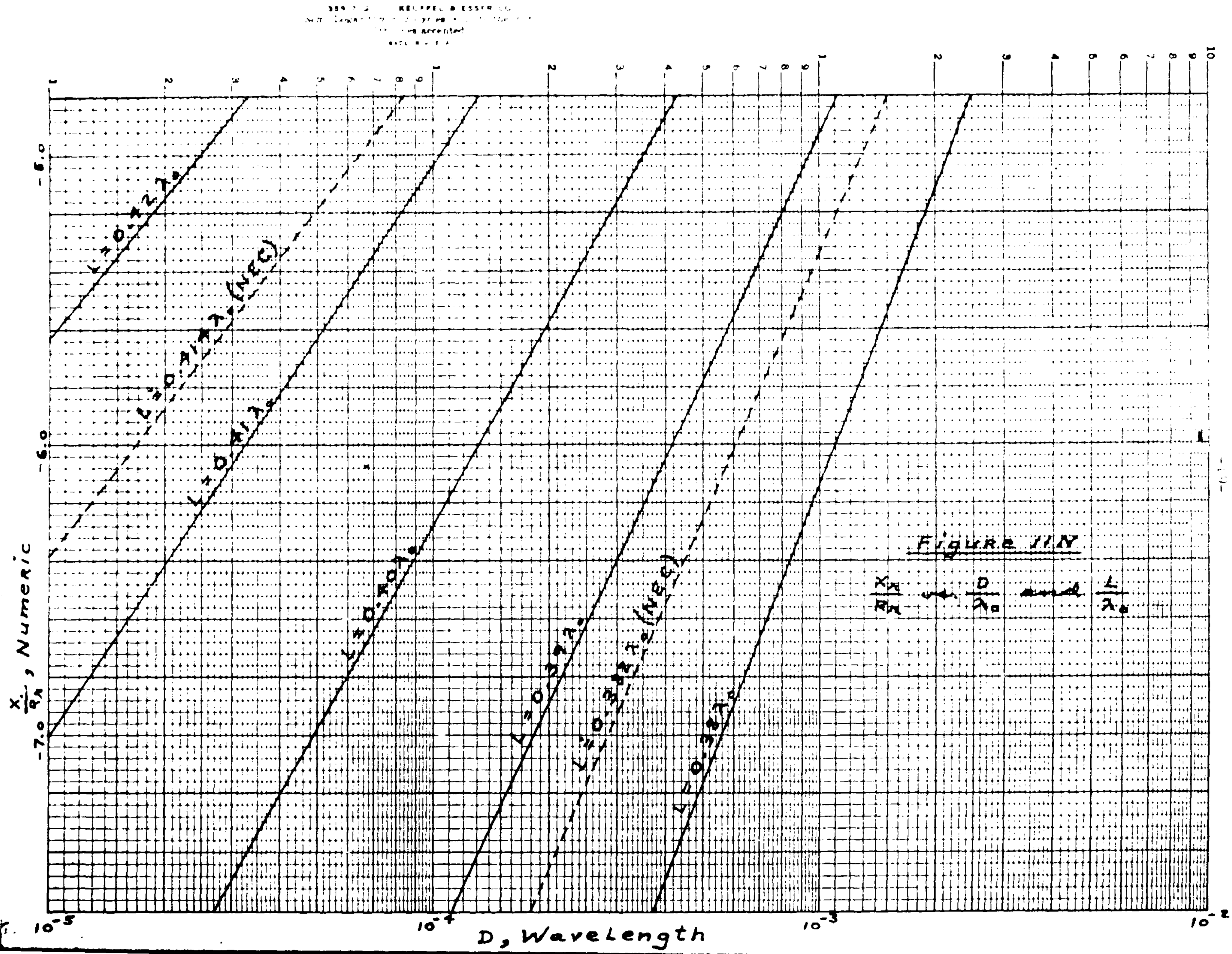
Figure 11N
$\frac{X_A}{R_A}$ vs $\frac{D}{\lambda_a}$ and $\frac{L}{\lambda_a}$
$\frac{X_A}{R_A}$, Numeric
D, Wavelength
-5.0
-6.0
-7.0
$10^{-5}$
$10^{-4}$
$10^{-3}$
$10^{-2}$

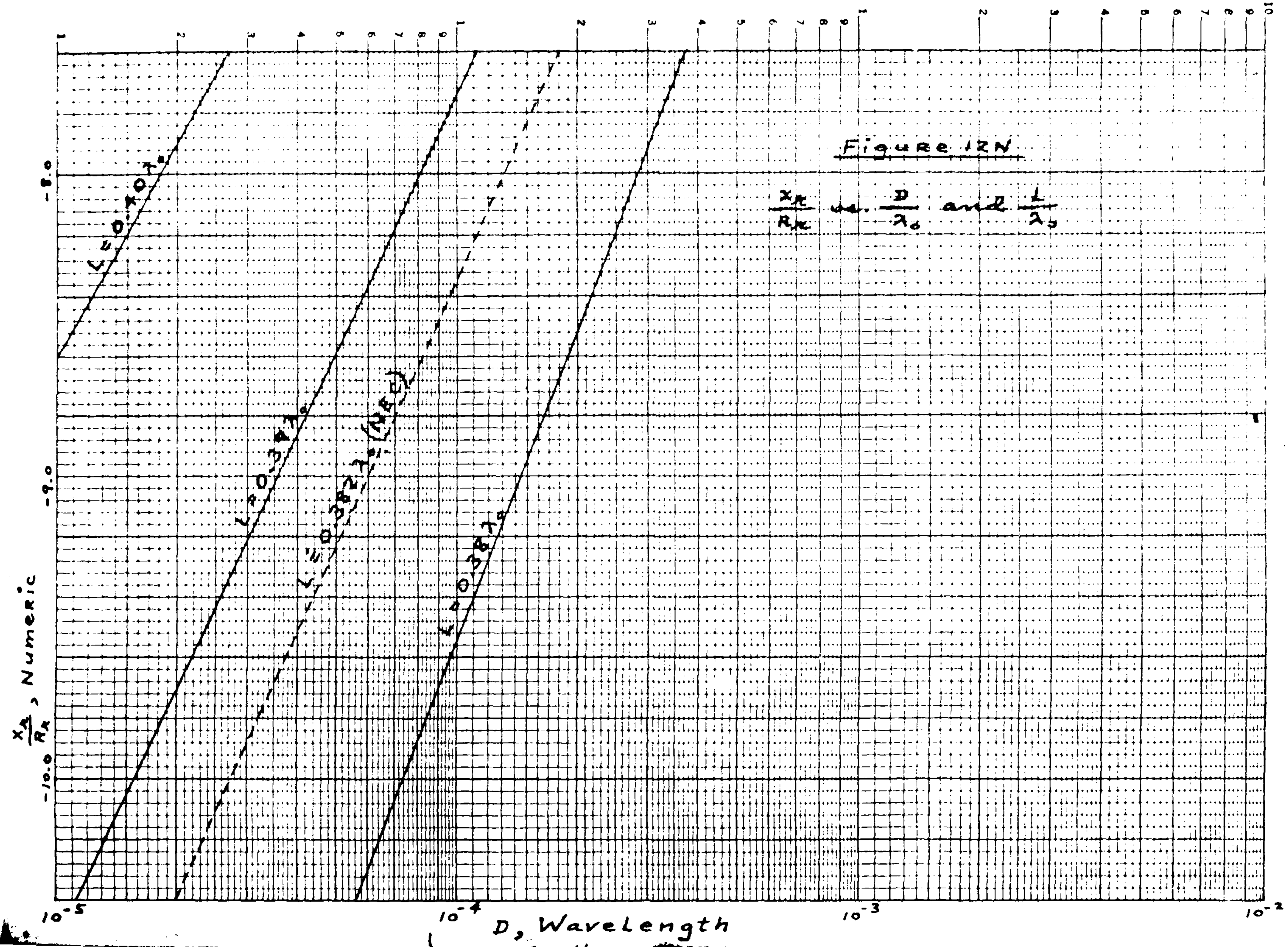


Figure 12N

$\frac{X_R}{R_R}$ vs. $\frac{D}{\lambda_s}$ and $\frac{L}{\lambda_s}$

## VI. SCALING EXAMPLES AND LIMITATIONS

In most cases, scaling involves a change in element diameter and a solution for element length while the $X_r/R_r$ ratio is held constant. Such solutions are not easily obtainable via equations 15 and 16. However, when these equations are plotted, as on Figures 3KM - 12N, graphical solutions can be obtained in a straightforward fashion. The one exception is when $X_r/R_r$ is independent of L/D (coefficients equal zero) in equations 15 and 16. This is a horizontal line with $L \doteq 0.4975\ \lambda_0$ plus $X_r/R_r \doteq 0.4311$ on Figure 4 KM, and $L \doteq 0.49966\ \lambda_0$ plus $X_r/R_r \doteq 0.5343$ on Figure 9N.

Calculations involving $0.41 < L < 0.42$ wavelengths in 0.01 wavelength increments plotted on Figures 5 KM and 10N show that vertical interpolation is not quite linear, but that linear interpolation gives good results. As an example, the dotted line on Figure 5 KM crosses the $D = 10^{-3}\lambda_0$ vertical line 41% of the vertical distance between $L = 0.41\lambda_0$ and $L = 0.42\lambda_0$ so that $L \doteq 0.4141\lambda_0$ via linear interpolation vs. $L \doteq 0.4140\lambda_0$ via equation 15 calculations vs. $L \doteq 0.4138\lambda_0$ ($\beta_0 h = 1.3$ radians) via King-Middleton data. As another example, the dotted line on Figure 10N crosses the $D = 4 \times 10^{-4}\lambda_0$ vertical line 37% of the vertical distance between $L = 0.41\lambda_0$ and $L = 0.42\lambda_0$ is $L \doteq 0.4137\lambda_0$ via linear interpolation vs. $L \doteq 0.4136\lambda_0$ via equation 16 calculations vs. $L \doteq 0.4138\lambda_0$ ($\beta_0 h = 1.3$ radians) via NEC calculations.

As a first example in the use of Figures 3KM - 12N, take a solid element which is first resonant at 47.6807 MHz when its length, $L_0$, is 2.95513125 meters (116 - 11/32 inches) and its diameter, $D_0$, is $3.81 \times 10^{-2}$ meters (1.5 inches), and one wishes to make a similar element from $2.54 \times 10^{-2}$ meters (1.0 inch) diameter, $D_\eta$, tubing. What should the new length, $L_\eta$, be?

Since this is a solid element, Figures 3KM - 7KM apply, and since it is first resonant $(X_r/R_r = 0)$, Figure 4KM is used. At 47.6807 MHz, $L_0 \doteq 0.47\lambda_0$, $D_0 \doteq 6.06 \times 10^{-3}\lambda_0$, and $(L_0/D_0) \doteq 77.5625$. When these values (using the relationship given in the Introduction) are used in equation 15, the solution $(X_r/R_r \doteq 0)$ agrees with point 1 on Figure 4KM.

In this example, the horizontal scaling line is $(X_r/R_r) = 0$. At 47.6807 MHz, the new diameter, $D_\eta$, is approximately $4.04 \times 10^{-3}\lambda_0$, and this is point 2 on Figure 4KM. Using linear vertical interpolation between $L = 0.47$ and $L = 0.48$ wavelengths on this figure, the solution for $L_\eta$ is approximately $0.4733\lambda_0$ or 2.97588 meters (117 - 5/32 inches) at 47.6807 MHz. This can be verified by using equation 15 $(E \doteq 6 \times 10^{-4})$.

As a second example in the use of Figures 3KM - 12N, take split series center-fed element which is first resonant at 49.6889 MHz when its total (both arms) length, $L_0$, is 2.8960 meters (114 inches) and its diameter, $D_0$, is $4.1148 \times 10^{-3}$ meters (#6 wire), and one wishes to make a similiar element from $1.2908 \times 10^{-3}$ meters (#16 wire) diameter, $D_\eta$, wire. What should the new length, $L_\eta$, be?

Since this is a split series center-fed element, Figures 8N - 12N apply, and since it is first resonant $(X_r/R_r = 0)$, Figure 9N is used. At 49.6889 MHz, $L_0 \doteq 0.48\lambda_0$, $D_0 \doteq 6.82 \times 10^{-4}\lambda_0$, and $(L_0/D_0) \doteq 703.8123$. When these values (using the relationship given in the Introduction) are used in equation 16, the solution $(X_r/R_r \doteq 0)$ aggrees with point 1 on Figure 9N.

In this example, the horizontal scaling line is $(X_r/R_r) = 0$. At 49.6889 MHz, the new diameter, $D_n$, is approximately $2.1394 \times 10^{-4}\lambda_0$, and this is point 2 on Figure 9N. Using linear vertical interpolation between $L = 0.48$ and $L = 0.49$ wavelengths on this figure, the solution for $L_n$ is approximately $0.4837\lambda_0$ or 2.91836 meters (114 - 29/32 inches) at 49.6889 MHz. This can be verified by using equation 16 $(E \doteq 10^{-3})$.

The purpose of using first resonance in these two examples is to show how well equations 2 and 4 compare with, respectively, equations 15 and 16 when $(X_r/R_r) = 0$. In the first example,

$$\frac{L_0}{D_0} \doteq \frac{2.95513}{0.0381} \doteq 77.5625 \qquad \text{numeric}$$

$$V_r \doteq 0.94147 \quad \text{(equation 2)} \qquad \text{numeric}$$

$$L_0 \doteq 0.94147 \left(\frac{\lambda_0}{2}\right) \doteq 0.47074\lambda_0 \qquad \text{wavelengths}$$

$$E_0 \doteq \frac{0.47074\lambda_0}{0.47\lambda_0} - 1 \doteq 0.157 \qquad \text{percent}$$

$$\frac{L_n}{D_n} \doteq \frac{2.97588}{0.0254} \doteq 117.1606 \qquad \text{numeric}$$

$$V_r \doteq 0.94708 \quad \text{(equation 2)} \qquad \text{numeric}$$

$$L_n \doteq 0.94708 \left(\frac{\lambda_0}{2}\right) \doteq 0.47354\lambda_0 \qquad \text{wavelengths}$$

$$E_n \doteq \frac{0.47354\lambda_0}{0.4733\lambda_0} - 1 \doteq 0.051 \qquad \text{percent}$$

In the second example,

$$\frac{L_0}{D_0} \doteq \frac{2.8960}{4.1148 \times 10^{-3}} \doteq 703.8009 \qquad \text{numeric}$$

$$V_r = 0.96013 \quad \text{(equation 4)} \qquad \text{numeric}$$

$$L_0 \doteq 0.96013 \left(\frac{\lambda_0}{2}\right) = 0.48007 \qquad \text{wavelengths}$$

$$E_0 \doteq \frac{0.48007\lambda_0}{0.48\lambda_0} - 1 \doteq 0.015 \qquad \text{percent}$$

$$\frac{L_n}{D_n} \doteq \frac{2.91836}{1.2908 \times 10^{-3}} \doteq 2260.8925 \qquad \text{numeric}$$

$$V_r \doteq 0.96713 \quad \text{(equation 4)} \qquad \text{numeric}$$

$$L_n \doteq 0.96713 \left(\frac{\lambda_0}{2}\right) \doteq 0.4836\lambda_0 \qquad \text{wavelengths}$$

$$E_n \doteq \frac{0.4837\lambda_0}{0.4836\lambda_0} - 1 \doteq 0.028 \qquad \text{percent}$$

These results are in excellent agreement near first resonance, and show why midrange comparison dotted lines are not necessary on Figures 3KM - 4KM or 8N - 9N.

It is often assumed that a single radiating element should be length-pruned to first resonance in order to be the most efficient center-fed dipole radiator. Theory and practice show that the maximum broadside gain of this configuration occurs when $L \doteq 1.25\lambda_0$, and its driving point impedance is complex inductive. Unfortunately, the driving point impedance is highly sensitive to length changes[2] when $L \doteq 1.25\lambda_0$ ($\beta_0 h \doteq 1.9635$ radians), and equations 15 - 16 are highly inaccurate when $L > 0.57\lambda_0$. The driving point impedance of this configuration is also relatively large[2], and highly sensitive to changes in mutual earth coupling impedance as well as changes in frequency. In this case, a versatile matching tuner is often required, and maximum expected gain may not be realized due to transfer losses. Hence, a first resonant element is generally used for bandwidth and matching reasons, and multi-element configurations are generally used to obtain higher gains.

When the radiating element is the driven element ($\ell_f$) of a Yagi-Uda type array, it is usually cut to first resonance, the reflector ($\ell_r$) is usually longer, and directors ($\ell_d$) are usually shorter to obtain a traveling-wave phenomenon.[3,6,7,8,9,10] As the references show, it is a rare case, indeed, where the passive elements lengths exceed the limits imposed upon equations 11 - 16 or upon Figures 3KM - 12N.

## VII. ELEMENT GAIN

Neither the mode theory data[1] nor the King-Middleton theory data[2] includes element gain. AMP and NEC calculations include solid angle gain, but the results are not conclusive. The first resonant AMP gain is too high ($\doteq 2.165$ dBi) when $(L/D) = 10^4$, and the first resonant NEC gain ($\doteq 2.115$ dBi) is independent of L/D when $40 \le (L/D) \le 10^4$! At the same time, both programs are sensitive to element length above and below first resonance.

Averaging the AMP and NEC gain figures over the $40 \le L/D \le 10^4$ and $1.2 \le \beta_0 h \le 1.8$ radians range, the following equation was derived:

$$G = 10^{p} \quad \text{dBi} \qquad 17$$

where,

$$p \doteq [0.1176-0.00276 \log_{10}(\tfrac{L}{D})](\beta_0 h)+0.0031 \log(\tfrac{L}{D})+0.1558 \quad \text{numeric}$$

As the coefficients indicate, normal diameter changes have little effect upon element gain. Over this range, $1.98 \le G \le 2.31$ dBi, with the greatest change at smaller (?) L/D ratios, and excellent correlation is obtained near NEC program first resonance ($E \doteq 0.01$ dB).

Equation 17 assumes that any antenna driving point reactance is tuned out by a lossless line matching network. This assumption is more realistic when the reactance is inductive than when the reactance is capacitive.

## VIII. SUMMARY

Equations 1 - 10 and Figures 1 - 2 are presented to show errors in mode theory, AMP program, and the Dr. Lawson theory. Equations 11 - 14 are presented so that scaled or unscaled element driving point impedance values can be obtained for transmission line matching network design. Equations 15 - 16 and Figures 3KM - 12N are presented to facilitate element scaling. Equation 17 is presented to give an estimated element gain vs. normalized dimensions.

The behavior of gain equation 17 is not what one would expect from theory. When solid elements are used, smaller L/D ratios usually give a lower Q (increased bandwidth)[2]. When split series-fed elements are used, the driving point impedance depends upon whose theory one is using, and Q is a function of impedance variations![11] Since equation 17 compromised gain, it also compromised Q and impedance variations vs. frequency (or wavelength) changes.

Figures 3KM - 12N answer a question that has been asked many times. The sensitivity of scaling to changes in L/D is a direct function of the difference between the element length and 0.5 (0.4975 for KM and 0.49966 for NEC) wavelength. This is reflected by change in lines slope on these figures. These lines also show the nonsymmetrical relationship between length changes when the length is less than 0.5

wavelength and length changes when the length is greater than 0.5 wavelength.

The scaling examples presented in Section VI assume no frequency change. When the dimensions are converted to normalized wavelength for use in Figures 3KM - 12N, the lengths and diameters apply to <u>any</u> frequency. For example, use Figures 3KM - 12N to scale from, say, 50 MHz to 2 MHz. The procedure is to calculate $L_0$ and $D_0$ in wavelength at 50 MHz, determine the horizontal $X_r/R_r$ scaling line on the appropriate figures, calculate a practical diameter in wavelength at 2 MHz, move along the constant $X_r/R_r$ horizontal scaling line on the figure to the 2 MHz diameter in wavelength, determine the new length in wavelength, and finally convert the new length to one of the basic units of measurement.

This analysis does not consider mutual coupling impedance between elements, or between a single element and another object such as ground. When the distance, S, between elements is equal to or greater than 3.0 wavelengths, mutual coupling impedance can generally be omitted when $0.40 \leq L \leq 0.55$ wavelength.[12,13] The same applies when the element height, H, over earth is greater than 1.5 wavelengths.[14] When the distance, S, between elements is held constant in <u>wavelengths</u>, L/D changes will have little effect upon existing mutual coupling impedance when $S \geq 20D$. The same applies for an element over earth when $H \geq 10D$. In almost all parallel or horizontal element examples, this condition is met, and mutual coupling impedance equations seldom include element diameter, D.

When highly conductive metallic elements are in proximity with each other, mutual coupling impedance solutions for $L \doteq 0.5$ wavelength can be obtained from solutions to Carter's closed-form exponential integrals.[15] These integrals assume a sinusoidal current distribution on (infinitely thin) elements, but they are reasonable approximations, and solutions are available in graphs and tables.[1,12,13,16] For greater accuracy, one is faced with solutions to integral representations of the Sommerfeld formulation.

When an antenna element is within 1.5 wavelengths of an imperfect earth, one is faced with solutions to the recalcitrant Sommerfeld formulation if realistic mutual coupling impedance values are to be obtained. Our AMP uses the Fresnel RCM (reflection-coefficient method) to determine mutual impedance, where the RCM is the leading term of a steepest descent method solution to infinite integrals. It has been pointed out that the RCM is valid ($E < 10\%$) only when all parts of the antenna element meet the following condition.[17]

$$H > \frac{0.7}{\sqrt{|e|}} \lambda_0 \qquad \text{meters} \qquad 18$$

Where H is the element height over the earth, $\lambda_0$ is the free-space wavelength and e is the earth's complex relative permittivity.

When two horizontal coplanar elements are near earth, it has been found that the RCM can be used to determine their mutual impedance when[18]

$$H > \frac{L}{5.5} \qquad \text{meters} \qquad 19$$

$$H \geq \frac{0.25}{\sqrt{|e|}} \lambda_0 \quad \text{wavelengths} \qquad 20$$

In this report, $0.40\lambda_0 \leq L \leq 0.55\lambda_0$ is the valid region for equations 15 - 16. Equation 19 is a mathematical pole ($\leq 90$ degrees) restriction which would be $0.10\lambda_0$ in this report. Over the HF region, $4.0 \leq |e| \leq 4.5 \times 10^4$ for most of the earths encountered, and equation 19 with $H > 0.10\lambda_0$ will be the RCM limiting height here.

Over the years, CCC-EMEO-PED personnel have used the AMP at heights which violated equations 18 - 20. The results were known to be incorrect, and a comparative report is available.[19] A reference 17 program error was discovered in this report, and it has since been corrected by AFCRL.[20] Nevertheless, enough information is available in that report to confirm equation 18, and verify field measurements.[21]

When the antenna height is below the equation 18 limit, one can use a semi-infinite integral representation of the Sommerfeld formulation, use the Gaussian interpolatory quadrature formula for obtaining solutions to the first integral, and use the Gaussian Laguerre interpolatory quadrature formula for obtaining solutions to the second integral. The formulations and justifications are lengthy, and are good approximations to heights, H, as low as $0.03\lambda_0$ where solutions become oscillatory.[22]

The work cited in reference 17 is similar to work done by Dr. E. Miller and his staff at the Lawrence Livermore Laboratory as a background in the preparation of the Sommerfeld subroutine of our new NEC program.

A review of new NEC data may show simplifications in the calculation of antenna-ground mutual coupling impedance.

I am indebted to Mr. W. Alvarez, Mr. D. Fink, and Mr. G. Lane of CCC-EMEO-PED for program data which made these observations possible. While the data is not precise, it is the best we have at this time.

* * * * * * * * * * * * * * * * * * * * * * * *

## REFERENCES

[1] S. Schelkunoff and H. Friis, Antennas: Theory and Practice, Chapter 13, John Wiley & Sons, Inc.; 1952.

[2] R. King, The Theory of Linear Antennas, pp. 168-182, Harvard University Press; 1956.

[3] J. Lawson, "Yagi Antenna Design," Ham Radio Magazine, pp. 22-27; January 1980.

[4] R. King and T. Wu, "Currents, Charges, and Near Fields of Cylindrical Antennas," Radio Sci. J. Res., Vol. 69D, No. 3, pp. 429-446; March 1965.

[5] Pointed out to me by Mr. George Lane of CCC-EMEO-PED from program users manuals.

[6] S. Uda and Y. Mushiake, Yagi-Uda Antenna, Sasaki Printing and Publishing Co. (Sendai, Japan), p. 110; 1954.

[7] L. Thourel, The Antenna, John Wiley & Sons, Inc., p. 140; 1960.

[8] H. Jasik, Antenna Engineering Handbook, McGraw-Hill Book Co., Inc., Chapter 5, p. 25; 1961.

[9] C. Chen and D. Cheng, "Optimum Element Lengths for Yagi-Uda Arrays," IEEE TRANS, AP-23, No. 1, pp. 8-15; January 1975.

[10] D. Kajfez, "Nonlinear Optimization Extends the Bandwidth of Yagi Antenna, " IEEE TRANS, AP-23, No. 2, pp. 287-289; March 1975.

[11] J. Ryder, Networks, Lines and Fields, Prentice-Hall, Inc., Second Edition, Chapter 2; 1955.

[12] F. Terman, Radio Engineers' Handbook, McGraw-Hill Book Co., Inc., p. 777; 1943.

[13] J.Kraus, Antennas, McGraw-Hill Book Co., Inc., p. 266; 1950.

[14] Ibid., p. 305.

[15] P. Carter, "Circuit Relations in Radiating Systems and Applications to Antenna Problems," PROC. IRE, Vol. 20, No. 6, pp. 1004-1041; June 1932.

[16] A. Hund, Short-wave Radiation Phenomena, Vol. I, McGraw-Hill Book Co., Inc., p. 696; 1952.

[17] T. Sarkar and B. Strait, "Analysis of Arbitrarily Oriented Thin Wire Antenna Arrays Over Imperfect Ground Planes," Syracuse University Scientific Report No. 9 (AFCRL-TR-75-0641), p. 32; December 1975.

[18] Ibid., p. 49

[19] H. Tolles, "Electrically-short Center-fed Horizontal Dipole Antennas for High-frequency Communications," EMEO-PED-77-8 (DDC No. ADA-047548); October 3, 1977.

[20] In a private discussion with Dr. Sarkar, he pointed out that it was a truncation error.

[21] E. Laport, Radio Antenna Engineering, McGraw-Hill Book Co., Inc., p. 238; 1952.

[22] T. Sarker and B. Strait, Op. Cit., Sections 2 and 3.

DATE
FILMED

8